Available online at www.sciencedirect.com
ScienceDirect
Ceramics International 34 (2008) 2085–2089
CERAMICS INTERNATIONAL
www.elsevier.com/locate/ceramint

Modelling of high-chromia refractory spalling in slagging coal gasifiers

R.E. Williford *, K.I. Johnson [1], S.K. Sundaram [2]

Pacific Northwest National Laboratory, Richland, WA 99352, USA

Received 3 May 2007; received in revised form 20 June 2007; accepted 12 August 2007
Available online 4 October 2007

Abstract

The economic viability of converting coal into clean burning liquid fuels in slagging coal gasifiers is compromised by the limited service lifetime of hot-face refractories. One of the most severe refractory degradation mechanisms is spalling, which can occur by either volume-expansion phenomena (compressive stresses) or by volume-shrinkage phenomena (tensile stresses). A volume-shrinkage model is benchmarked to high-chromia refractory material properties and performance under gasifier operating conditions. The model is found to be appropriate for first-order estimates of gasifier refractory lifetime when the apparent diffusivity of volatized Cr in the refractory includes the effects of slag-filled pores and cracks.

Keywords: B. Failure analysis; B. Interfaces; C. Mechanical properties; E. Refractories

1. Introduction

Coal conversion into clean burning liquid fuels promises environmental advantages and reduced dependence on oil. However, these advantages have not been fully realized because of an important economic factor: the limited service lifetime of hot-face refractories [1,2]. Under optimum conditions in a slagging coal gasifier, high-chromia refractories could last up to 3.5 years [3]. However, commercial gasifiers must often use sub-optimal feedstocks and operating conditions, and the refractory lifetime is often reduced to less than 1.5 years. The expense of refractory replacement in a large-scale gasifier can exceed US$1 million [1]. Consequently, one of the most frequently cited R&D needs [2] is for improved refractory durability, including improved models for refractory lifetime prediction.

The challenging service conditions in a slagging coal gasifier include high temperatures (1300–1600 °C) and pressures (2–3 MPa), temperature transients and the associated thermal stresses, alternating oxidizing and reducing conditions, corrosive slags, and erosive residual particulates. Although additions of phosphate [4], magnesia [5], or alumina [6] to high-chromia refractories have exhibited measured improvements in durability, industrial refractories have a finite amount of porosity, including initial flaws and joints between bricks. These enable penetration of the slag into the interior of the refractory by permeation and infiltration mechanisms assisted by the pressure gradients within the gasifier, along with capillary and diffusive intrusion mechanisms. The thermal–chemical–mechanical interactions between the refractory and slag result in degradation by several mechanisms: corrosion, erosion, cracking, and spalling. Spalling is one of the most difficult to predict because of its apparent stochastic nature.

Several types of spalling models have appeared in the literature, e.g., [7–15]. The driving forces that cause spalling fall into two regimes: those that cause refractory volume expansion and those that cause volume shrinkage [16]. Aside from the obvious thermal expansion, other expansion mechanisms include phase changes resulting from slag-refractory chemical reactions. Expansion causes compressive stresses in the plane of the refractory surface, which lead to sub-surface cracking, and the eventual formation of a 'blister' configuration that spalls [17]. Shrinkage mechanisms can include the loss of volatile species, e.g., Cr [18] or chemically bound water, from the refractory

* Corresponding author at: Mail Stop K2-44, Pacific Northwest National Laboratory, Richland, WA 99352, USA. Tel.: +1 509 375 2956; fax: +1 509 375 2186.
E-mail address: Rick.Williford@pnl.gov (R.E. Williford).
[1] Present address: Mail Stop K5-22, Pacific Northwest National Laboratory, Richland, WA 99352, USA.
[2] Present address: Mail Stop K6-24, Pacific Northwest National Laboratory, Richland, WA 99352, USA.

0272-8842/$34.00
doi:10.1016/j.ceramint.2007.08.011

matrix. Shrinkage leads to tensile stresses in the plane of the refractory surface, and the eventual formation of a crack system resembling a dried up clay riverbed. The cracked refractory segments form spalled regions when they are removed by the flowing slag or by gravity.

We have previously discussed a model of spalling by volumetric expansion mechanisms [17]. The purpose of the present work is to explore the application of a shrinkage-based model [19] for representative gasifier conditions and materials, and to determine if it can adequately estimate observed spall sizes and times to spall. The present volume-shrinkage spalling model, along with the previous volume-expansion model, will be used to help guide fundamental understanding, testing, and data collection in our research program on coal gasification.

2. Spalling by volume-shrinkage mechanisms

Yakobson [19] previously derived a model for the tensile cracking of a homogeneous solid as solutes or other volatile species are removed. Fig. 1 shows a schematic of the crack network that results from the volume shrinkage of the host material. The volatile species diffuses through the solid with diffusivity D (cm^2/s), and escapes from the cracked/solid interface according to a rate constant k (cm/s). The apparent diffusivity may be increased by the crack network near the cracked/solid interface, so transport away from the interface is usually rapid. The mean crack length at the interface is L (cm), and defines the mean size of the spalled material. The lower diagram in Fig. 1 shows the concentration profile of the volatile species, with the cracked/solid interface moving into the solid at mean velocity v (cm/s). The concentration of the diffusing species is normalized to that in the initial solid, with c_b being the normalized concentration at the cracked/solid interface. Note that although a relatively large cracked region is shown in Fig. 1, the spalled material is most likely to be carried away by the flowing slag in a gasifier, or to fall away from the surface due to gravitational forces.

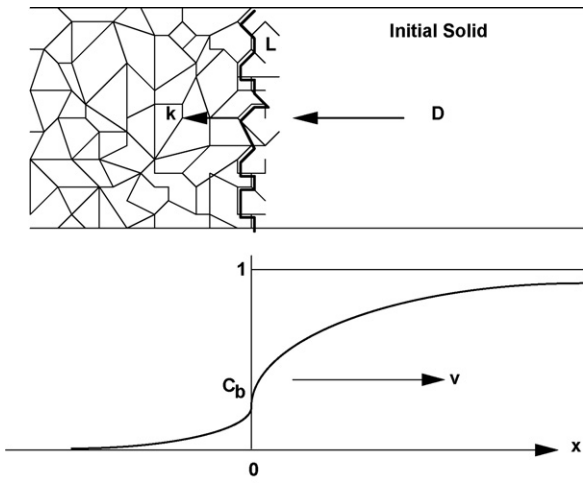

Fig. 1. Top diagram: crack network propagating towards the interior of the solid at velocity v. Bottom diagram: concentration profile of volatile species leaving the solid at the cracked/solid interface ($x = 0$). Redrawn from Ref. [19].

Yakobson's model describes the competition between crack opening forces due to material shrinkage and crack resisting forces due to material cohesion. Because diffusion is slower than the growth of an unstable crack, the stress $\sigma(x)$ is balanced by the material toughness (K), and the system is considered to be in quasiequilibrium. K is given by fracture mechanics as [20]:

$$K = 2\sqrt{\frac{L}{\pi}}\int_0^{\mathrm{L}} \frac{\sigma(x)}{\sqrt{(L^2 - x^2)}}\mathrm{d}x \tag{1}$$

The system is just balanced when K takes the critical value K_c. In terms of material constants, K_c is given by fracture mechanics as [20]:

$$K_c = \frac{2\Gamma E}{\sqrt{(1 - \nu_p^2)}} \tag{2}$$

where Γ is the material surface energy (J/m^2), E the Young's modulus (N/m^2), and ν_p is the Poisson's ratio.

The stress distribution in the plane of the refractory surface was approximated from thermal stress theory [21], neglecting the effects of crack curvature and crack interactions

$$\sigma(x) = \beta E[1 - c(x)] \tag{3}$$

where

$$\beta = \frac{\Delta V}{3V(1 - \nu_p)} \tag{4}$$

is the volume-shrinkage coefficient and $\Delta V/V$ is the volume shrinkage normalized to the initial volume.

The steady-state concentration profile $c(x)$ of the diffusing species in the moving coordinate system is defined by the concentration at the cracked/solid interface (c_b)

$$c(x) = 1 - (1 - c_b)\,\mathrm{e}^{-xv/D} \tag{5}$$

and can be approximated by the linear form

$$c(x) \cong c_b + x(1 - c_b)\frac{v}{D} \tag{6}$$

for $x \leq D/v$. Substituting Eqs. (2), (3), and (6) into Eq. (1) gives

$$\frac{K_c}{2E\beta}\left(1 + \frac{v}{k}\right)\sqrt{\frac{\pi v}{D}} = \sqrt{\lambda}\left(\frac{\pi}{2} - \lambda\right) \tag{7}$$

where the dimensionless length is defined as

$$\lambda = \frac{vL}{D} \tag{8}$$

The normalized length of the crack (λ) depends on the velocity (v) of the crack front propagation.

The solution to Eq. (7) is given by a family of possible crack velocities, so the problem is one of 'selection'. According to Yakobson [19], the critical velocity occurs at the maximum value of the crack elastic opening force, where the gradient of a corresponding free energy functional is zero. Identifying the critical velocity as v_c, Yakobson solved for the critical dimensionless length $\lambda_c = \pi/6$, and from Eq. (8) found the

characteristic crack (or spall) size as a function of velocity: $L = \pi D/6v$. Substituting this into Eq. (7) gives the characteristic equation

$$v\left(1+\frac{v}{k}\right)^2 = \Delta \tag{9}$$

where the coefficient Δ is determined by the material properties

$$\Delta = \frac{2D}{27}\left(\frac{E\beta\pi}{K_c}\right)^2 \tag{10}$$

Eqs. (9) and (10) provide the model to be investigated here. This model has been verified by Monte Carlo simulations [22] for cases of high and low diffusivity.

3. Benchmarking for gasifier applications: Cr volatization in high-chromia refractories

There are several possible mechanisms by which a refractory may exhibit volume shrinkage, such as post-sintering densification or loss of chemically bound water during initial dryout. Slagging gasifier operating conditions include high temperatures and a harsh chemical environment. The chemistry is often very complicated, so it is problematic to select a suitable case for benchmarking the candidate model described above. In the interest of clarity, we have selected Cr volatization because (a) Cr volatization creates vacancies in the Cr_2O_3 lattice, which in turn cause volume shrinkage, (b) it has been observed in slagging gasifier refractories [18], and (c) it is a problem common to other technologies [23].

The materials database employed was the same as in our previous volume-expansion model [17]. Young's modulus (E) for a typical high-chromia refractory was estimated as $E = 2 \times 10^{11}$ Pa [24] at room temperature. The correction for higher temperatures ($1 - 0.0002T$), with T in °C, was estimated from Richerson [25]. The correction for porosity $(1-p)^2$ from Gibson and Ashby [26] was employed, with porosity $p = 0.15$ typical of high-chromia refractories [18,24]. The in situ operating value was thus estimated as $E = 1 \times 10^{11}$ Pa. The value of Poisson's ratio was taken as $\upsilon_p = 0.25$ [25]. The crack extension force, i.e., the force per unit width of crack front required to advance the crack length was estimated from the surface energy to be about $\Gamma = 10$ J/m^2 [27]. K_c was calculated from Eq. (2).

Spalling data for benchmarking the model were also the same as for benchmarking our previous volume-expansion model [17]. Because of the harsh operating conditions, in situ data are extremely rare, and not often cited in the literature. At the average operating temperature of ~1450 °C, spall times of 807 h [28] and 1300–1500 h [16] have been observed. We assumed 1000 h as a typical time to spall. Spall thicknesses of 1–3 cm on the average were reported by Guo et al. [28]. Although experimental conditions were not reported in Ref. [16], the brick used in Ref. [28] was taken from a Texaco gasifier after being cycled 20 times between 1350 and 1700 °C in a Qiwu coal and limestone feed mixture.

The volume shrinkage caused by Cr volatization was calculated with an atomistic energy minimization method [29] using several sets of interatomic potentials. The most reliable potentials were those of Sun et al. [30,31]. Other potentials [32] employed the more elaborate core–shell models and were unstable at Cr vacancy concentrations greater than 2%. An example is shown in Fig. 2. In all simulations, charge neutrality was maintained by adjusting the charge on the Cr cations. The correlation for volume shrinkage ($\Delta V/V$) as a function of the Cr vacancy fraction (V_{Cr}) in Cr_2O_3, derived using the Sun et al. [30,31] potentials, was used in this benchmarking exercise

$$\frac{\Delta V}{V} = -0.45512 V_{Cr} \tag{11}$$

Results are shown in Fig. 2. For a high-chromia refractory (designated CR95 in Ref. [18]), we assumed that the shrinkage would be dominated by the Cr_2O_3, which is actually 92.5% of the refractory material. Effects of the porosity on the mechanical properties were treated as described above [26].

The rate constant k was computed using the conservation of mass equation for the diffusing species at the cracked/solid boundary

$$v(1 - c_b) = kc_b \tag{12}$$

Taking c_b as the normalized Cr concentration (c_{Cr}) at the cracked/solid interface, and noting that $c_{Cr} = 1 - V_{Cr}$, we have

$$k = v\frac{V_{Cr}}{1 - V_{Cr}} \tag{13}$$

The cubic form of Eq. (9) was solved numerically [33], keeping only the single real root. Results are shown in Fig. 3 for a range of V_{Cr}. For $D = 10^{-6}$ cm^2/s, the benchmark spalling data (a 1.4 cm thick spall in 1000 h) are matched for $V_{Cr} \sim 0.023$ (i.e.,

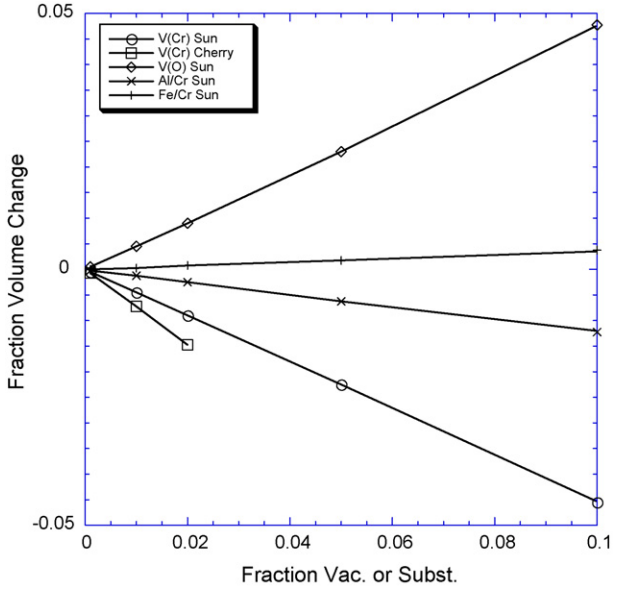

Fig. 2. Volume change normalized by original Cr_2O_3 crystal volume for a range of vacancies and substitutions. Cr vacancies and Al_{Cr} substitutions cause shrinkage, while O vacancies and Fe_{Cr} substitutions cause expansion. References for the interatomic potentials are indicated in the legend.

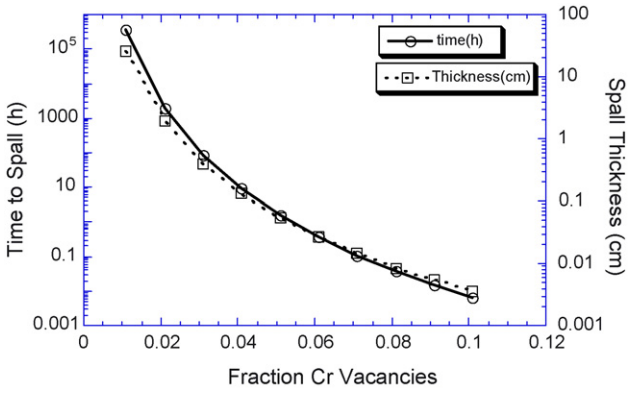

Fig. 3. Time to spall and spall thickness for a range Cr vacancy concentrations in Cr_2O_3, with $D = 10^{-6}$ cm^2/s. At $V_{Cr} \sim 0.023$, a spall ~1.4 cm thick is obtained in ~1000 h.

2.3%), a reasonable defect level for a ceramic subjected to a complex chemical environment at high temperatures. This model is therefore model capable of reproducing observed spalling data using representative refractory material properties.

Fig. 4 shows the times to spall for a range of diffusivities at the defect level $V_{Cr} = 0.023$. The rapid increase in spall times with decreasing diffusivity would seem to indicate that higher diffusivities are appropriate for porous and cracked refractories, or that the pore and microcrack networks appear to play an important role in Cr diffusion through the refractory for spalling by volume-shrinkage mechanisms.

4. Discussion and conclusions

Because of the complexity of slag/refractory chemical interactions, identification of an appropriate benchmarking case was problematic. We chose the relatively simple and clear case of volume shrinkage caused by Cr volatization because it has been observed to occur in high-chromia refractories [18].

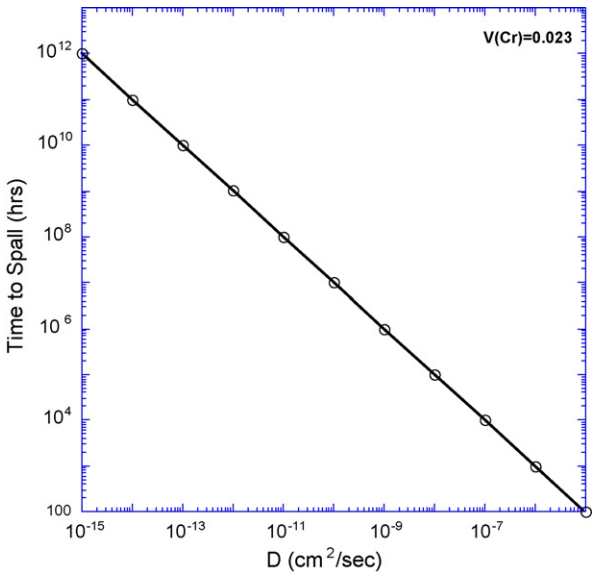

Fig. 4. Dependence of time to spall on the effective diffusivity of Cr in the refractory, for 2.3% Cr vacancies.

Although Yakobson [19] assumed that the cracks at the interface do not strongly influence the diffusion of the volatile species, our analysis shows that application to refractories gives results agreeing with available benchmark spalling data only if the apparent diffusivity in the cracked solid is relatively high (~10^{-6} cm^2/s). This is much higher than the diffusivity of Cr through the Cr_2O_3 crystal lattice (10^{-10} to 10^{-18} cm^2/s at 1450 °C) [34–37]. However, it is representative of the diffusivity of metal atoms through liquid slags [38] and implies that the slag-filled pores and cracks of the refractory must play an important role in Cr diffusion. This would in turn imply that the Cr volatization process could occur mostly at the surfaces of the pores and cracks, where the refractory interacts chemically with the slag. Although this is physically reasonable, it also means that the volume shrinkage may actually be less than that given in Eq. (11) for homogeneous Cr_2O_3, so the time to spall may be longer. It is thus apparent that further refinements are needed in the model. Such refinements include the possible 'pore surface confinement' of the volume-shrinkage coefficient and the treatment of the assumed 'homogeneous' host refractory as a composite for the stress analysis. We plan to generate data relevant for assessing the magnitude of these affects in our experimental program.

The above model is investigated for possible use in large-scale gasifier simulations, so its computational conciseness and simplicity are attractive. It is essentially a three-parameter model. The primary input data needed are the diffusivity, the toughness, and the volume-shrinkage coefficient. The model treats elastic behavior and does not account for creep or other stress relaxation phenomena. Although it is approximate, the model's computational uncertainties are considered to be comparable to the uncertainties for the in situ refractory material properties and the gasifier chemical environment. Thus, the model appears useful as a first-order estimate for refractory lifetime predictions for volume-shrinkage phenomena.

Acknowledgements

This work was supported by the PNNL Laboratory Directed Research and Development Program (Energy Conversion Initiative). Pacific Northwest National Laboratory is operated for the US Department of Energy (DOE) by Battelle Memorial Institute under contract DE-AC06-76RLO-1830. The authors would like to acknowledge the support and guidance of George Muntean and Mike Elliott of PNNL.

References

[1] S.J. Clayton, G.J. Siegel, J.G. Wimer, U.S. Department of Energy Report, DOE/FE-0447, 2002.
[2] G.J. Stiegel, Overview of gasification technologies, ACERC Technical Conference at BYU, Provo, Utah, http://www-cerc.byu.edu/News/, February, 16–17, 2006.
[3] M.E. Fahrion, Materials testing at cool water coal-gasification plant, Mater. High Temp. 11 (1993) 107–112.
[4] C.P. Dogan, K.-S. Kwong, J.P. Bennett, R.E. Chinn, C.L. Dahlin, New developments in gasifier refractories, in: Proceedings of the Gasification Technologies Conference, San Francisco, October, 27–30, 2002.

[5] A. Rezaie, W.L. Headrick, W.G. Fahrenholtz, R.E. Moore, M. Valez, W.A. Davis, Interaction of refractories and alkaline containing corrodants, Refract. Appl. News 9 (5) (2004) 26–31, Special issue on Refractories for Gasifiers, September/October.
[6] J.P. Bennett, K.-S. Kwong, Refractory liner materials used in slagging gasifiers, Refract. Appl. News 9 (5) (2004) 20–25, Special issue on Refractories for Gasifiers September/October.
[7] E. Chen, O. Buyukozturk, Thermomechanical behavior and design of refractory linings for slagging gasifiers, Am. Ceram. Soc. Bull. 64 (1985) 988–994.
[8] C.A. Schacht, Refractory Linings, Marcel Dekker, Inc., 1995.
[9] J.A. Sweeney, M. Cross, Analyzing the stress response of commercial refractory structure in service at high temperatures. II A thermal stress model for refractory structures, Trans. J. Br. Ceram. Soc. 81 (1982) 47–52.
[10] O. Buyukozturk, T. Tseng, Thermomechanical behavior of refractory concrete linings, J. Am. Ceram. Soc. 65 (1982) 301–307.
[11] J. Rawers, J. Kwong, J. Bennett, Characterizing coal gasifier slag-refractory interactions, Mater. High Temp. 16 (1999) 219–222.
[12] E. Chen, Simulation of the thermomechanical behavior of monolithic refractory lining in coal gasification environment, Radex Rundschau 4 (1990) 376–384.
[13] K. Andreev, H. Harmuth, FEM simulation of the thermo-mechanical behavior and failure of refractories—a case study, J. Mater. Process. Technol. 143–144 (2003) 72–77.
[14] S. Yilmaz, Thermomechanical modelling for refractory lining of a steel ladle lifted by crane, Steel Res. 74 (2003) 485–490.
[15] X. Liang, W.L. Headrick, L.R. Dharani, Continuum damage mechanics modelling of the failure of refractory cup under thermal loading and chemical shrinkage, Refract. Appl. News 11 (2006) 17–23.
[16] K.-S. Kwong, J. Bennett, R. Krabbe, C. Powell, Engineered refractories for slagging gasifiers, Am. Ceram. Soc. Bull. 85 (2) (2006) 17–20.
[17] R.E. Williford, K.I. Johnson, S.K. Sundaram, A refractory spalling model for slagging coal gasifiers, Ceram. Int., submitted for publication.
[18] P. Biedenkopf, T. Karwath, D. Kobertz, M. Rane, E. Wessel, K. Hilpert, L. Singheiser, Vaporization, Corrosion of refractories in the presence of pressurized pulverized coal combustion slag, J. Am. Ceram. Soc. 84 (2001) 1445–1452.
[19] B.I. Yakobson, Morphology and rate of fracture in chemical decomposition of solids, Phys. Rev. Lett. 76 (12) (1991) 1590–1593.
[20] M.F. Kanninen, C. Popelar, Advanced Fracture Mechanics, Oxford University Press, 1985.
[21] S.P. Timoshenko, J. Goodier, Theory of Elasticity, McGraw-Hill, New York, 1970.
[22] A. Malthe-Sorenssen, B. Jamtveit, P. Meakin, Fracture patterns generated by diffusion controlled volume changing reactions, Phys. Rev. Lett. 96 (2006) 245501.
[23] N. Sakai, T. Horita, K. Yamaji, Y.P. Xiong, H. Kishimoto, M.E. Brito, H. Yokokawa, Material transport and degradation behavior of SOFC interconnects, Solid State Ionics 177 (2006) 1933–1939.
[24] Z.Q. Guo, Refractories for gasifiers, Bull. Am. Ceram. Soc. (2004) 9101–9108.
[25] D.W. Richerson, Modern Ceramic Engineering, Marcel Dekker, Inc., New York, 1992.
[26] L.J. Gibson, M.F. Ashby, Cellular Solids: Structure and Properties, 2nd ed., Cambridge University Press, Cambridge, UK, 1997.
[27] W.D. Kingery, H.K. Bowen, D.R. Uhlman, Introduction to Ceramics, Wiley & Sons, New York, 1976, p. 183.
[28] Z.Q. Guo, B.Q. Han, H. Dong, Effect of coal slag on the wear rate and microstructure of the ZrO_2-bearing chromia refractories, Ceram. Int. 23 (1997) 489–496.
[29] J.D. Gale, GULP, A computer program for the symmetry-adapted simulation of solids, J. Chem. Soc., Faraday Trans. 93 (1997) 629–637.
[30] J. Sun, T. Stirner, A. Matthews, Calculation of native defect energies in alpha-Al_2O_3 and alpha-Cr_2O_3 using a modified Matsui potential, Surf. Coat. Technol. 201 (2006) 4201–4204.
[31] J. Sun, T. Stirner, W.E. Hagston, A. Leyland, A. Matthews, A simple transferable interatomic potential model for binary oxides applied to bulk alpha-Al_2O_3 and the (0 0 0 1) alpha-Al_2O_3 surface, J. Cryst. Growth 290 (2006) 235–240.
[32] R.E. Williford, T.R. Armstrong, J.D. Gale, Chemical and thermal expansion of calcium-doped lanthanum chromite, J. Solid State Chem. 149 (2000) 320–326.
[33] S. Wolfram, Mathematica, Addison-Wesley Publishing, Reading, MA, 1998,, p. 692.
[34] A.C.S. Sabioni, B. Lesage, A.M. Huntz, J.C. Pivin, C. Monty, Self-diffusion in Cr_2O_3. I. Chromium diffusion in single crystals, Phil. Mag. A 66 (1992) 333–350.
[35] A.C.S. Sabioni, A.M. Huntz, F. Millot, C. Monty, Self-diffusion in Cr_2O_3. II. Oxygen diffusion in single crystals, Phil. Mag. A 66 (1992) 351–360.
[36] A.C.S. Sabioni, A.M. Huntz, F. Millot, C. Monty, Self-diffusion in Cr_2O_3. III. Chromium and oxygen grain boundary diffusion in polycrystals, Phil. Mag. A 66 (1992) 361–374.
[37] A.M. Huntz, J. Balmain, S.C. Tsai, K. Messoudi, M.K. Loudjani, B. Lesage, J. Li, Diffusion studies in oxide scales grown on alumina and chromia-forming alloys, Scripta Mater. 37 (1997) 651–660.
[38] V.D. Eisenhuttenleute, Slag Atlas, 2nd ed., Verlag Stahleisen GmbH, 1995